ELectronics EXpress
IEICE Electronics Express, Vol.19, No.13, 1–6
LETTER

Application of new sliding mode control in vector control of PMSM

Hao Yang[1]**, Jing-Wei Tang**[2, a)]**, and Ying-Ren Chien**[3]

Abstract Aiming at the characteristics of low observation accuracy and high chattering of traditional sliding mode observers (SMO), a new SMO is proposed to reduce chattering and improve accuracy. In PMSM vector control, PI control has the problems of poor anti–disturbance ability and speed pulsation, while the traditional sliding mode control (SMC) has the problem of serious chattering, Therefore, on this basis, an SMC based on the new reaching law is designed, and the simulation is carried out in Matlab/Simulink. The simulation results show that the improved SMO has better performance and stronger stability than the traditional SMO. At the same time, compared with the traditional SMC and PI control, the SMC based on the new reaching law can make it respond well when the motor target speed changes suddenly, and effectively improve the problem of traditional SMC chattering, The control accuracy and steady-state error of the PMSM system are improved.

Keywords: sliding mode observer (SMO), new reaching law, permanent magnet synchronous motor (PMSM), vector control, no position sensor Sliding mode control (SMC)
Classification: Power devices and circuits

1. Introduction

PMSM has been widely used in industry because of its high control accuracy and high–power factor [1, 2, 3, 4, 5].

In PMSM operation control, the encoder is required to collect rotor speed information, but mechanical sensors have problems such as difficult installation and maintenance and high cost. Therefore, a large number of scholars have paid extensive attention to and applied research on Sensorless Speed Estimation Algorithm in PMSM [6, 7, 8, 9, 10]. At present, several main sensorless algorithms are SMO, neural network, and high-frequency signal injection. Among them, the SMO is not affected by the parameters of the motor itself and has strong robustness. Compared with the other two methods, this method has more significant advantages in speed sensorless control systems. The essence of the sliding mode observer is state reconstruction, which uses the known data of the system as the input to estimate the output value of the actual system. In PMSM vector control, the essence of SMO is to quickly modify the value of back EMF by using a high-frequency switching signal, so that the estimated current is equal to the actual current, and obtain the rotor speed information through the observed back EMF. However, because of the characteristics of symbolic functions and other voltage and current noise, the system chattering will be caused. At present, the method of weakening the chattering of sliding mode observers is the mainstream research direction [13, 14, 15, 16]. Reference [17] proposed the design idea of using fractional-order sliding mode surface and phase-locked loop and designed a new saturation function to weaken chattering. In reference [18], a super torque SMO is proposed by using the sliding mode coefficient varying with the speed. The simulation results show that the observation error can be reduced by 25%. In reference [19], the frequency adaptive composite coefficient filter is used to replace the low-pass filter in the design of SMO, which is verified by simulation.

In addition, because PMSM is a nonlinear system, the conventional PI control can not meet its needs of it [20, 21, 22, 23]. SMC has advantages in nonlinear control. However, due to the discontinuity of its control, high-frequency switching movement near the sliding mode surface will produce a chattering problem [24, 25, 26, 27, 28]. Reference [29] designed a new sliding mode reaching law to reduce chattering and dynamically change the speed reaching the sliding mode surface. Literature [30] combines the extended state observer with sliding mode control, takes the system load disturbance as feedforward compensation, and proposes an adaptive sliding mode controller. The experimental results show that the proposed controller can effectively reduce chattering and improve system performance. However, the suppression of SMC external disturbance and parameter change is realized by setting a large switching gain, which will lead to the chattering phenomenon, which needs to be avoided in the actual system.

Given the serious chattering phenomenon and low observation accuracy in the traditional sensorless algorithm, a new piecewise saturation function is used to replace the switching function. Based on the traditional exponential reaching law, an adaptive sliding mode reaching law is designed. On this basis, this paper designs an adaptive sliding mode speed controller for sensorless PMSM speed regulation system and compares it with the traditional PI and sliding mode speed controller in Matlab/Simulink. The simulation results show that the proposed method has a fast response, small chattering and strong robustness.

2. Mathematical model of PMSM

To make our control more simple, here we assume that the three-phase symmetrical distribution of stator winding, electromagnetic symmetry, ignoring the iron loss and unsatu-

[1] Anhui Technical College of Mechanical and Electrical Engineering, An hui, 241002, China
[2] Hunan College of Information, Hunan, 410200, China
[3] Department of Electrical Engineering, National Ilan University, Yilan City, 26041, Taiwan, R.O.C.
a) tang2021048@163.com

DOI: 10.1587/elex.19.20220156
Received March 25, 2022
Accepted April 5, 2022
Publicized June 15, 2022
Copyedited July 10, 2022

rated magnetic circuit, ignoring the influence of temperature and other factors on the flux linkage of a permanent magnet. The mathematical model of PMSM is transformed into the following mathematical model through Clark and Parker transformation [29-30].

$$L_s\left(\frac{di_a}{dt}\right) = -R_s i_a - e_a + u_a \tag{1}$$

$$L_s\left(\frac{di_\beta}{dt}\right) = -R_s i_\beta - e_\beta + u_\beta \tag{2}$$

$$e_\alpha = -\psi_f \omega_r \sin\theta \tag{3}$$

$$e_\beta = \psi_f \omega_r \cos\theta \tag{4}$$

$$T_e = \frac{3}{2} p i_q \left[i_d\left(L_d - L_q\right) + \psi_f\right] \tag{5}$$

$$J\frac{d\omega_r}{dt} = T_e - T_L - B\omega_r \tag{6}$$

Where J is the moment of inertia, i_α and i_β are the stator current under α-β, R_s is the stator resistance, u_α and u_β are the stator voltage under α-β, L_s is the inductance of stator winding, L_d and L_q are d-q axis inductance, e_α and e_β are the back electromotive force under α-β, ψ_f is the flux linkage of the permanent magnet; θ is the electrical angle, ω_r is the angular speed of the motor rotor, T_e is electromagnetic torque, T_L is the load torque, B is the friction coefficient, p is the polar logarithm.

3. Design of a new SMO

3.1 Design of traditional SMO

Among many sensorless control strategies, SMO is widely used because it is simple, insensitive to parameter changes, and independent of specific models. The mathematical model of traditional SMO is as follows:

$$L_s\frac{d\hat{i}_\alpha}{dt} = -R_s\hat{i}_\alpha - k_1 sign\left(\hat{i}_\alpha - i_\alpha\right) + u_\alpha \tag{7}$$

$$L_s\frac{d\hat{i}_\beta}{dt} = -R_s\hat{i}_\beta - k_1 sign\left(\hat{i}_\beta - i_\beta\right) + u_\beta \tag{8}$$

$\hat{i}_\alpha$, $\hat{i}_\beta$ is the estimated value of current. $\hat{u}_\alpha$, $\hat{u}_\beta$ is the estimated value of voltage. k_1 is the gain of the SMO.

Subtract equations 1 and 2 from equations 7 and 8 to obtain:

$$L_s\left(\frac{d\hat{i}_\alpha}{dt} - \frac{di_\alpha}{dt}\right) = -R_s\left(\hat{i}_\alpha - i_\alpha\right) - k_1 sign\left(\hat{i}_\alpha - i_\alpha\right) + e_\alpha \tag{9}$$

$$L_s\left(\frac{d\hat{i}_\beta}{dt} - \frac{di_\beta}{dt}\right) = -R_s\left(\hat{i}_\beta - i_\beta\right) - k_1 sign\left(\hat{i}_\beta - i_\beta\right) + e_\beta \tag{10}$$

When the estimated value is equal to the actual value, the system reaches the sliding mode surface. At this time, according to the dynamic conditions of the SMC theory:

$$e_\alpha = k_1 sign\left(\hat{i}_\alpha - i_\alpha\right) \tag{11}$$

$$e_\beta = k_1 sign\left(\hat{i}_\beta - i_\beta\right) \tag{12}$$

The resulting back EMF contains the position information of the motor rotor, so after filtering, the following can be obtained:

$$\theta = -\arctan\frac{e_\alpha}{e_\beta} \tag{13}$$

$$\omega_e = \frac{d\theta}{dt} \tag{14}$$

Where θ is the electrical angle; ω_e is the electrical angular velocity.

The structure of the traditional SMO is shown in Fig. 1.

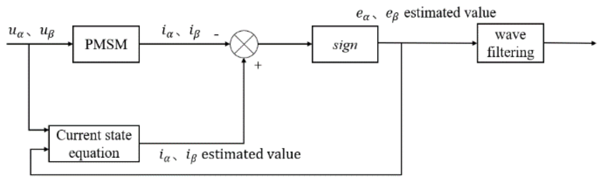

Fig. 1 Structure diagram of traditional SMO.

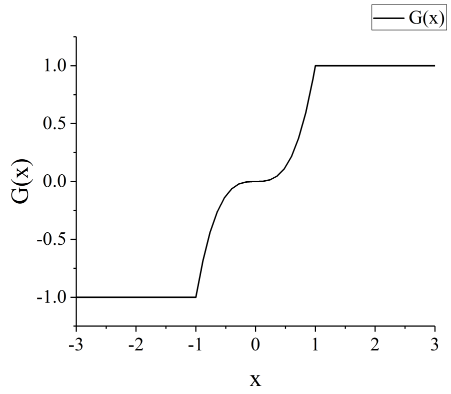

Fig. 2 Saturation function G(x) when the boundary layer thickness is 1.

3.2 SMO based on new switching function

To reduce the system chattering caused by the symbolic switching function, a new piecewise saturation function is proposed.

The new saturation function G(x) is:

$$G(x) = \begin{cases} \frac{x^3}{\sigma^3}, |x| \le \sigma \\ sign(x), |x| > \sigma \end{cases} \tag{15}$$

Where x is the error between the observed current value and the actual value, and σ is the thickness of the boundary layer. When σ is equal to 1, the function image is shown in Fig. 2 below. It can be seen that there is the characteristic of error saturation outside the thickness of the boundary layer, and the exponential change of the function within the thickness of the boundary layer can make the observation of back EMF more stable.

It can be deduced that the mathematical model of the new observer is:

$$L_s\frac{d\hat{i}_\alpha}{dt} = -R_s\hat{i}_\alpha - k_2 G\left(\hat{i}_\alpha - i_\alpha\right) + u_\alpha \tag{16}$$

$$L_s\frac{d\hat{i}_\beta}{dt} = -R_s\hat{i}_\beta - k_2 G\left(\hat{i}_\beta - i_\beta\right) + u_\beta \tag{17}$$

When the $\hat{i}_\alpha = i_\alpha$, it can be obtained that the back EMF is:

$$e_\alpha = k_2 G\left(\hat{i}_\alpha - i_\alpha\right) \tag{18}$$

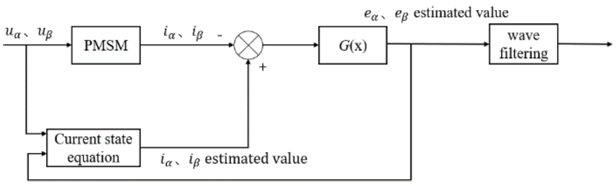

Fig. 3 Structure diagram of new SMO.

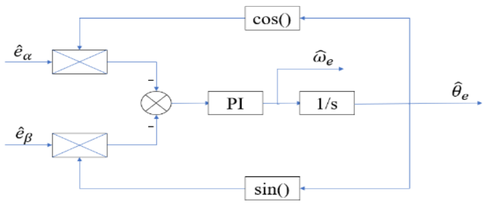

Fig. 4 Structure diagram of PLL.

$$e_\beta = k_2 G\left(\hat{i}_\beta - i_\beta\right) \tag{19}$$

k_2 is the gain of the new SMO.

The new SMO is shown in Fig. 3 below.

Considering the influence of inverter switching, load disturbance, controller saturation, and other factors, the direct use of the arctangent method to extract speed information will reduce the estimation accuracy. Therefore, the PLL system is designed to extract the speed information. The specific implementation is shown in Fig. 4.

In Fig. 4, the phase synchronization is realized through the phase-locked loop phase feedback control to ensure that the controlled frequency accurately tracks the input signal frequency, which is used to solve the phase error in the rotor angle estimation caused by the filter. The back EMF containing rotor error information outputs the rotor speed signal through PI regulation, and the estimated position of the rotor is obtained through the integration link.

4. Sliding mode controller based on new reaching law

4.1 Design of the new SMC

Due to the nonlinearity of PMSM, the conventional PI control can not meet the needs of the system. In PMSM vector control, SMC is used to replace the traditional PI speed controller, which can effectively improve the control accuracy and anti–disturbance ability of the system.

Define the state variables in PMSM as:

$$\left.\begin{aligned} x_1 &= \omega_{ref} - \omega_r \\ x_2 &= \frac{dx_1}{dt} = \frac{d\omega_{ref}}{dt} - \frac{d\omega_r}{dt} \end{aligned}\right\} \tag{20}$$

$$\dot{x}_1 = x_2 = \frac{d\omega_{ref}}{dt} - \frac{1}{J}\left(-T_L + \frac{3}{2}p\psi_f i_q - B\omega_r\right) \tag{21}$$

The integral sliding surface is adopted, and the sliding surface is defined as:

$$s = c\int_0^t e dt + e \tag{22}$$

Where c is greater than 0.

$$e = \omega_{ref} - \omega \tag{23}$$

e is the error between the rated motor speed and the actual motor speed.

The traditional exponential approach law is:

$$S = \dot{s} = -\varepsilon sign(s) - qs, \varepsilon, q > 0 \tag{24}$$

Bring into equation (22) above:

$$\dot{s} = -\varepsilon sign(s) - qs = ce + \dot{e} \tag{25}$$

The q-axis current can be obtained as:

$$i_q = \frac{2}{3p\psi_f}\left[T_L + B\omega - J\left(\dot{s} - ce\right)\right] \tag{26}$$

Although it has a certain disturbance ability and control performance. However, using the traditional exponential reaching law, there will be serious chattering, which increases the switching frequency and burden of the controller. Therefore, an SMC based on the adaptive adjustment of the reaching law parameters of the system state is proposed to improve its anti–disturbance ability and performance of it.

The new approach law is:

$$\dot{s} = -\varepsilon(1-\alpha)sign(s) - ke^{|s|}s \tag{27}$$

$$\alpha = \begin{cases} e^{-e|s|}, & |s| < 1 \\ 1 - e^{|s|}, & |s| \geq 1 \end{cases} \tag{28}$$

4.2 Proof of stability

The Lyapunov function is used to analyze the stability of the designed new reaching law sliding mode speed controller. Firstly, the Lyapunov function is defined:

$$V(s) = \frac{1}{2}s^2 \tag{29}$$

By deriving it, we get:

$$\dot{V}(s) = s\dot{s} = s\left(-\varepsilon|s|^\alpha sgn(s) - ks\right) \tag{30}$$

$$\dot{V}(s) = -\varepsilon s|s|^\alpha sgn(s) - ks^2 \tag{31}$$

It can be seen from the above formula that $V(s)$ is positive definite, $\dot{V}(s)$ is negative definite. Due to this, the designed new SMC can achieve stability and ensure that the system enters the sliding mode state.

4.3 Performance analysis

The classical system is used to compare the new reaching law designed in this paper with the traditional exponential reaching law to verify the performance of the two reaching laws.

$$\dot{x}(t) = ax(t)^2 + u(t) \tag{32}$$

Where a = 5, u is the controller. The integral sliding surface is adopted, and the sliding surface function is defined as:

$$s = c\int_0^t e dt + e \tag{33}$$

The tracking error is:

$$e = x_d - x, \dot{e} = \dot{x}_d - \dot{x} \tag{34}$$

Where is the given target signal, $x_d = \sin t$

$$\dot{s} = ce + \dot{e} = c\left(x_d - x\right) + \left(\dot{x}_d - ax^2 - u\right) = S \tag{35}$$

S is the reaching law. At this time, the expression of sliding mode controller is:

$$u(t) = c\left(x_d - x\right) + \dot{x}_d - ax^2 - S \tag{36}$$

Table I Two parameters of approach law.

TERL	NARL
ε=5	ε=5
q=10	k=10

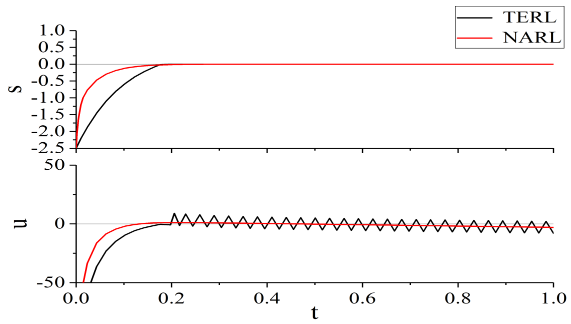

Fig. 5 Time-varying curve of controller u and sliding surface function s.

The traditional exponential reaching law (TERL) sliding mode controller and the new adaptive reaching law (NARL) sliding mode controller are simulated in Matlab/Simulink. The results are shown in Fig. 5, and the controller parameters are shown in Table I.

From the simulation results, it can be seen that the SMC based on the NARL can suppress chattering better than the TERL, and the reaching speed is fast in convergence.

5. Simulation verification

In this paper, the PMSM Vector Control Based on SMC is simulated by Matlab/Simulink, and the control mode of id = 0 is adopted. The parameters are: permanent magnet flux linkage $\psi_f = 0.175$ WB, stator resistance $R_s = 3.578\,\Omega$, $L_d = L_q = 0.0085$ H, p=4, moment of inertia $J = 0.008\,\text{kg·m}^2$. The target speed suddenly changes from 400 r/min to 600 r/min at 0.6 s. The PMSM vector topology is shown in Fig. 6 below.

As shown in Fig. 7 below, a is the speed estimation of the traditional SMO and B is the speed estimation of the new SMO. Fig. 8 shows the comparison of the speed errors of the two observers.

From Fig. 7 and Fig. 8 that the precision of the new SMO is higher than that of the traditional SMO. The error of the traditional SMO changes sharply within −5∼10 r/min, while the chattering of the SMO with the new saturation function is significantly weakened, and the speed error changes gently, almost zero.

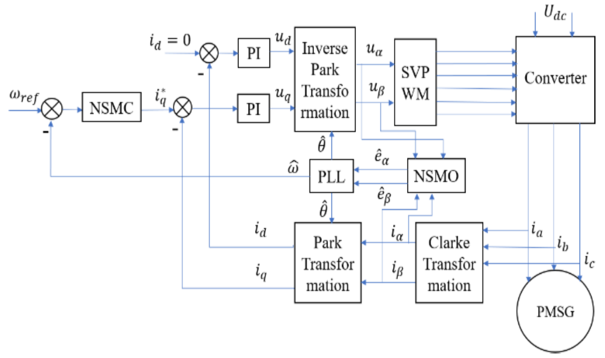

Fig. 6 PMSM vector topology.

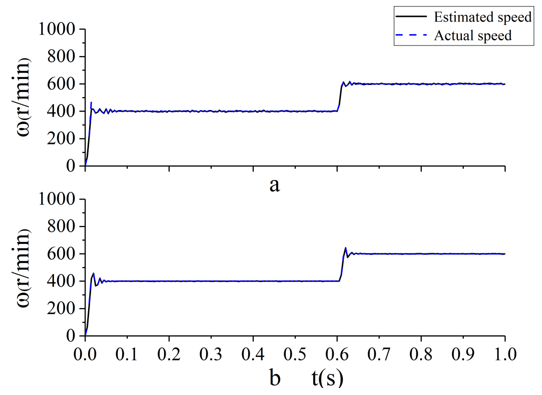

Fig. 7 Speed comparison of two observers.

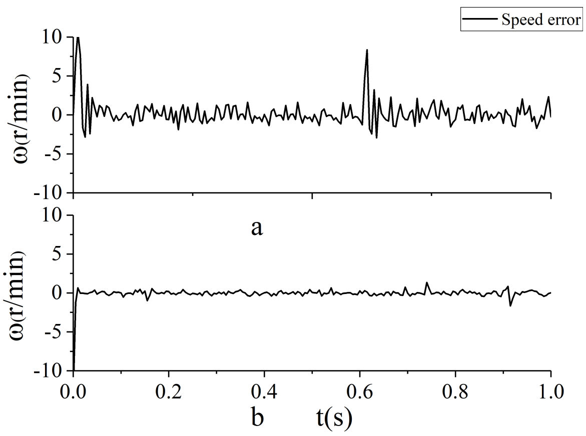

Fig. 8 Error comparison of two observers.

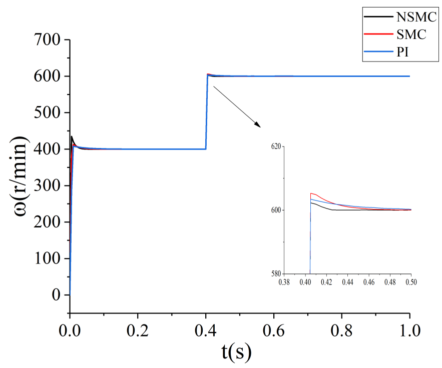

Fig. 9 Comparison of speed regulation effects of three controllers.

The following Fig. 9 shows the comparison of simulation results of three control modes: SMC, PI, and new sliding mode controller (NSMC).

As can be seen from Fig. 9, when the target speed changes suddenly at 0.4 s, the response times of PI, SMC, and NSMC are 0.07 s, 0.051 s, and 0.018 s respectively. Through comprehensive numerical analysis, compared with the existing methods, the proposed NSMC has a faster transient response, faster chattering suppression, and stronger anti–disturbance ability.

To further verify the robustness of the new sliding mode controller, set the simulation time as 0.2 S, the target speed as 400 r/min, and suddenly $T_L = 0.6$N·m at 0.6 s, and the simulation results are shown in Fig. 10 below.

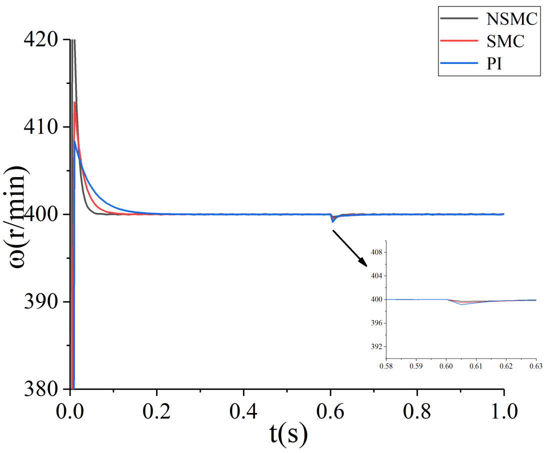

Fig. 10 Comparison of three control methods when loading torque changes.

As can be seen from Fig. 10, when the load torque changes suddenly, the time for the motor speed to recover to the actual value under the three control modes is 0.06 s, 0.12 s, and 0.19 s respectively. It shows that the proposed new sliding mode controller has good anti disturbance ability.

6. Conclusion

Aiming at the problems of observation accuracy of traditional SMO in PMSM speed regulation system and the serious chattering problem of traditional SMC in vector control, a new SMO based on new saturation function is established, and a new reaching law SMC with self-adaptive regulation ability is designed, Thus, the problems existing in the operation of PMSM are effectively suppressed. Theoretical analysis and simulation verify the feasibility and effectiveness of the algorithm.

Acknowledgments

This work is supported by the 2022 Academic Support Project for Top Talents of Anhui University Subjects (Specialties).

References

[1] L. Zhang, *et al.*: "Speed sensor-less control system of surface-mounted permanent magnet synchronous motor based on adaptive feedback gain supertwisting sliding mode observer," Journal of Sensors **2021** (2021) 8301359 (DOI: 10.1155/2021/8301359).

[2] L. Zhang, *et al.*: "Fast-super-twisting sliding mode speed loop control of permanent magnet synchronous motor based on SVM-DTC," IEICE Electron. Express **18** (2020) 20200375 (DOI: 10.1587/elex.17.20200375).

[3] L. Zhang, *et al.*: "SPMSM sliding mode control based on the new super twisting algorithm," Complexity **2021** (2021) 2886789 (DOI: 10.1155/2021/2886789).

[4] J. Cao, *et al.*: "Optimal control strategy of state feedback control for surface-mounted PMSM drives based on auto-tuning of seeker optimization algorithm," International Journal of Applied Electromagnetics and Mechanics **66** (2021) 705 (DOI: 10.3233/jae-201630).

[5] D. Bobba, *et al.*: "Multi-physics based analysis and design of stator coil in high power density PMSM for aircraft propulsion applications," AIAA Propulsion and Energy 2021 Forum (2021) (DOI: 10.2514/6.2021-3306).

[6] J. Ding, *et al.*: "Research on sensorless control of permanent magnet synchronous motor based on adaptive sliding mode observer," 2021 4th International Conference on Circuits, Systems and Simulation (ICCSS) (2021) (DOI: 10.1109/iccss51193.2021.9464214).

[7] Z.H. Wang, *et al.*: "Speed sensorless control of permanent magnet synchronous motor based on robust adaptive algorithm," Journal of Physics: Conference Series **1754** (2021) 012104 (DOI: 10.1088/1742-6596/1754/1/012104).

[8] X. Xia, et al.: "High precision low-speed control for permanent magnet synchronous motor," Sensors **20** (2020) 1526 (DOI: 10.3390/s20051526).

[9] Y. Belkhier, *et al.*: "Robust interconnection and damping assignment energy-based control for a permanent magnet synchronous motor using high order sliding mode approach and nonlinear observer," Energy Reports **8** (2022) 1731 (DOI: 10.1016/j.egyr.2021.12.075).

[10] W. Abd El Maguid Ahmed, *et al.*: "PSO technique applied to sensorless field-oriented controlPMSM drive with discretized RL-fractional integral," Alexandria Engineering Journal **60** (2021) 4029 (DOI: 10.1016/j.aej.2021.02.049).

[11] X. Liu, *et al.*: "SMO-based sensorless control of a permanent magnet synchronous motor," Front. Energy Res. (2022) 10:839329 (DOI: 10.3389/fenrg.2022.839329).

[12] S. Murshid and B. Singh: "An improved SMO for position sensorless operation of PMSM driven solar water pumping system," 2020 IEEE International Conference on Power Electronics, Smart Grid and Renewable Energy (PESGRE) (2020) (DOI: 10.1109/PESGRE45664.2020.9070426).

[13] Q. An, *et al.*: "Frequency-adaptive complex-coefficient filter-based enhanced sliding mode observer for sensorless control of permanent magnet synchronous motor drives," IEEE Trans. Ind. Appl. **56** (2019) 335 (DOI: 10.1109/tia.2019.2951760).

[14] A. Teklu, *et al.*: "A new frequency adaptive second-order disturbance observer for sensorless vector control of interior permanent magnet synchronous motor," IEEE Trans. Ind. Electron. **68** (2021) 11847 (DOI: 10.1109/tie.2020.3047065).

[15] L. Tung, *et al.*: "Exponential reaching law sliding mode control for dual arm robots," Journal of Engineering Science and Technology **15** (2020) 2841.

[16] C. Napole, *et al.*: "A global integral terminal sliding mode control based on a novel reaching law for a proton exchange membrane fuel cell system," Applied Energy **301** (2021) 117473 (DOI: 10.1016/j.apenergy.2021.117473).

[17] Y. Huang and F. Wu: "A sensorless control method for permanent magnet synchronous motor based on fractional-order sliding mode observer," 2020 IEEE 5th Information Technology and Mechatronics Engineering Conference (ITOEC) (2020) (DOI: 10.1109/itoec49072.2020.9141772).

[18] Y. Zhan, *et al.*: "An adaptive second-order sliding-mode observer for permanent magnet synchronous motor with an improved phase-locked loop structure considering speed reverse," Transactions of the Institute of Measurement and Control **42** (2020) 1008 (DOI: 10.1177/0142331219880712).

[19] Q. An, *et al.*: "Frequency-adaptive complex-coefficient filter-based enhanced sliding mode observer for sensorless control of permanent magnet synchronous motor drives," IEEE Trans. Ind. Appl. **56** (2019) 335 (DOI: 10.1109/tia.2019.2951760).

[20] L. Zhou, *et al.*: "Research on vector control of permanent magnet synchronous motor of high precision turntable based on fuzzy neural network," 2020 3rd International Conference on Electron Device and Mechanical Engineering (ICEDME) (2020) (DOI: 10.1109/icedme50972.2020.00034).

[21] P. Thamizhazhagan and S. Sutha: "Adaptive vector control reference strategy based speed and torque control of permanent magnet synchronous motor," Microprocessors and Microsystems **74** (2020) 103007 (DOI: 10.1016/j.micpro.2020.103007).

[22] S. Rubino, *et al.*: "Modular vector control of multi-three-phase permanent magnet synchronous motors," IEEE Trans. Ind. Electron. **68** (2021) 9136 (DOI: 10.1109/tie.2020.3026271).

[23] D. Huang, *et al.*: "Modeling and control of internal oscillations in energy-synchronous direct antenna modulation," (2021).

[24] X, Lei, *et al.*: "Global fast terminal sliding mode controller of permanent magnet synchronous motor," Micromotors (2013).

[25] Z. Qiao, *et al*.: "New sliding-mode observer for position sensorless control of permanent-magnet synchronous motor," IEEE Trans. Ind. Electron. **60** (2013) 710 (DOI: 10.1109/tie.2012.2206359).
[26] D.E. Chaouch: "Application of passivity-based and sliding mode control of permanent magnet synchronous motor under controlled voltage," Journal of Vibration and Control **28** (2021) 2022 (DOI: 10.1177/1077546321989507).
[27] T. Li and X. Liu: "Model-free non-cascade integral sliding mode control of permanent magnet synchronous motor drive with a fast reaching law," Symmetry **13** (2021) 1680 (DOI: 10.3390/sym13091680).
[28] P. Gao, *et al*.: "An adaptive super twisting nonlinear fractional order PID sliding mode control of permanent magnet synchronous motor speed regulation system based on extended state observer," IEEE Access **8** (2020) 53498 (DOI: 10.1109/access.2020.2980390).
[29] Q. Wang, *et al*.: "An improved sliding mode control using disturbance torque observer for permanent magnet synchronous motor," IEEE Access **7** (2019) 36691 (DOI: 10.1109/access.2019.2903439).
[30] P. Xia, *et al*.: "Speed adaptive sliding mode control with an extended state observer for permanent magnet synchronous motor," Mathematical Problems in Engineering **2018** (2018) 1 (DOI: 10.1155/2018/6405923).
[31] K. Zhang, *et al*.: "Field enhancing model predictive direct torque control of permanent magnet synchronous machine," IEEE Trans. Energy Convers. **36** (2021) 2924 (DOI: 10.1109/TEC.2021.3070339).
[32] A. Teklu, *et al*.: "A new frequency adaptive second-order disturbance observer for sensorless vector control of interior permanent magnet synchronous motor," IEEE Trans. Ind. Electron. **68** (2021) 11847 (DOI: 10.1109/tie.2020.3047065).